Supporting Information for

One Collision – Two Heteroatoms: Gas Phase Preparation of Azasilabenzene

Surajit Metya,[a] Iakov A. Medvedkov, [a] Shane J. Goettl, [a] Tosaporn Sattasathuchana,* [b], Mateus X. Silva[c,d], Breno R. L. Galvão,* [c] Ralf I. Kaiser*[a]

---

[a] Dr. S. Metya, Dr. Iakov A. Medvedkov, S. J. Goettl, Prof. Dr. R. I. Kaiser
Department of Chemistry
University of Hawai'i at Manoa
Honolulu, HI 96822 (USA)
E-mail: ralfk@hawaii.edu

[b] Dr. T. Sattasathuchana
Department of Chemistry
University of Hawai'i at Manoa
Honolulu, HI 96822 (USA)
E-mail: tsatta@hawaii.edu

[c] Dr. B R. L. Galvão, Dr. Mateus X. Silva
Centro Federal de Educação Tecnológica de Minas Gerais
Belo Horizonte 30421-169, Brazil
E-mail: brenogalvao@gmail.com

[d] Dr. Mateus X. Silva
Present Address:
Departamento de Química
Universidade Federal de Ouro Preto, Campus Morro do Cruzeiro
Ouro Preto, Minas Gerais 35402-136, Brasil

Experimental methods

The gas-phase reaction between silicon nitride (SiN, $X^2\Sigma^+$) and 1,3-butadiene (C_4H_6, X^1A_g) was investigated under single-collision conditions using a crossed molecular beam apparatus. While the experimental procedure is detailed elsewhere,[1-3] a brief overview is provided here. The supersonic beam of silicon nitride (SiN, $X^2\Sigma^+$) was generated in situ via laser ablation of a silicon rod using the 266 nm output of a Nd:YAG laser (2 mJ/pulse, 30 Hz, Quanta-Ray) in the presence of nitrous oxide (N_2O), which served both as a reactant and carrier gas. The silicon nitride (SiN, $X^2\Sigma^+$) seeded supersonic N_2O beam was formed using a 60 Hz piezoelectric (Parker–Hannifin/Proch–Trickl) pulsed valve, operated at -400 V with a backing pressure of 4 atm. After passing through a skimmer, the pulsed molecular beam is chopped using a four-slot chopper wheel to select a specific velocity distribution, resulting in a peak velocity (v_p) of 1189 ± 16 m s^{-1} and a speed ratio (S) of 4.4 ± 0.4. A second, perpendicular supersonic beam of 1,3-butadiene was generated using a similar 60 Hz Proch–Trickl pulsed valve, with a backing pressure of 550 Torr of pure gas. This beam exhibited a peak velocity (v_p) of 790 ± 12 m s^{-1} and a speed ratio (S) of 9.5 ± 0.3. Based on the velocities of the primary (SiN) and secondary (C_4H_6) beams, the collision energy was determined to be 24 ± 0.5 kJ mol^{-1}. The reaction products were detected in the plane of the intersecting beams using time-of-flight (TOF) mass spectrometry with a rotatable, triply differentially pumped "universal" detector. In this setup, neutral product species entering the detector chamber were first ionized by a Brink-type electron ionizer operating at 80 eV with an emission current of 1.8 mA.[4] The resulting ions were mass-filtered according to their mass-to-charge (*m/z*) ratios using a quadrupole mass spectrometer (QMS, Extrel, 1.2 MHz), and subsequently detected by a Daly-type particle ion counter in ultra-high vacuum (7×10^{-12} Torr).[5] TOF spectra were collected at laboratory angles ranging from 25.75° to 55.75° with respect to the primary silicon nitride beam, in 5° increments. Instantaneous background correction was applied to the TOF spectra by operating the laser at half the pulse valve frequency, ensuring accurate and reliable data collection.

The laboratory (LAB) angular distribution and time-of-flight (TOF) spectra were transformed into the center-of-mass (CM) reference frame using a forward convolution routine to extract detailed information about the reaction dynamics.[6, 7] This method begins with initial guesses for the angular flux distribution, $T(\theta)$, and the translational energy distribution, $P(E_T)$, in the CM frame. These distributions are then convoluted with the apparatus function to simulate TOF spectra and LAB angular distributions. The process is iterated until the simulated data achieves the best fit with the experimental results. The final output of the experiments is a product flux contour map, which represents the reactive differential cross section, denoted as $I(\theta, u)$. This quantity describes the intensity of reactively scattered products as a function of the scattering angle (θ) and the product center-of-mass velocity (u). The intensity can be expressed as $I(\theta, u) \sim P(u) \times T(\theta)$, where $P(u)$ is the velocity distribution and $T(\theta)$ is the angular distribution of the scattered products.

Computational methods

Electronic structure calculation

The geometries of the intermediates, transitions states and reaction products were obtained by performing electronic structure calculations with the ORCA[8] package using the double-hybrid density functional B2PLYP[9] including the atom-pairwise dispersion correction with the Becke-Johnson damping scheme (D3BJ)[10, 11] and the def2-TZVPP[12] basis set. At this level, we also performed a vibrational analysis to obtain the harmonic frequencies and zero-point energies of each structure and performed intrinsic reaction coordinate calculations for the transition states to confirm their connections.

In addition, nucleus independent chemical shielding (NICS)[13, 14] was calculated at B2PLYP/def2-TZVPP using the Gauge-Independent Atomic Orbital (GIAO)[15] method to characterize the degree of aromaticity of the products.[16] All NICS calculations were performed by using the optimized structures at B2PLYP-D3(BJ)/def2-TZVPP level of theory.

To enhance the accuracy of the relative energy of all structures, we performed single-point energy calculations using the explicitly correlated version of the coupled-cluster singles and doubles plus perturbative triples (CCSD(T)-F12)[17, 18] method, with the cc-pVTZ-F12[19] basis set. This energy refinement has been carried out using the MOLPRO[20] software.

Quasi-Atomic Orbital Analysis of $SiNC_4H_5$ Isomers

To elucidate the nature of chemical bonds in **p1-3** in the present work, the quasi-atomic orbital (QUAO) analysis was employed. Briefly, quasi-atomic orbitals can be thought of as distorted atomic minimal basis set orbitals resulting from the bonding formation in a molecule.[21-26] The QUAO analysis provides quantitative information about the types of bonding interaction, electron populations, bond order (BO), and the kinetic bond order (KBO), which indicates the strength of chemical bonding.[24, 26, 27] **Table S4** demonstrates KBOs and BOs of QUAO pairs of **p1-3**, while the percentages of s and p characters and electron populations from QUAO analysis are tabulated in **Table S5**. The QUAO at each atom center is labelled as follows:

- The first letter is the atomic symbol on which the orbital is located.
- If the QUAO participates in bonding, the symbol of a complementary atom is listed as a subscript.
- The Greek letter indicates the bonding types, e.g., σ and π orbitals.
- If the QUAO electron populations are close to 2, they are a lone pair (lp).

For example, $N_{C_4Si\pi}$ is a π QUAO located on N atom which is oriented towards C_4 and Si. The reference of atom numbers in **Table S4** and **S5** are displayed in **Figure S3**.

Table S1. Peak velocities (vp) and speed ratios (S) of the Silicon Nitride radical (SiN) and 1,3-butadiene (C_4H_6) beams along with the corresponding collision energies (EC) and center-of-mass angles (Θ_{CM})

Beam	v_p (m s^{-1})	S	E_c (kJ mol^{-1})	Θ_{CM} (degree)
Silicon nitride Radical (SiN)	1189 ± 16	4.4 ± 0.4		
1,3 Butadiene (C_4H_6)	790 ± 12	9.5 ± 0.3	24 ± 0.5	40.25 ± 0.4

Rice−Ramsperger−Kassel−Marcus (RRKM) Calculation:

The Rice–Ramsperger–Kassel–Marcus (RRKM) theory[28, 29] was used to calculate microcanonical, energy-dependent rate constants for all unimolecular reaction steps on the potential energy surface (PES) for the reaction of silicon nitride and 1,3-butadiene. These calculations were performed using our in-house code Unimol,[30] which evaluates rate constants as functions of internal energy under the harmonic approximation. Unimol is an improved version of our earlier software for computing energy-dependent RRKM rate constants for multiwell and multichannel unimolecular reactions under single-collision conditions. It also solves first-order kinetic equations.[31] In these calculations, the internal energy is taken as the sum of the collision energy and chemical activation energy, equivalent to the negative of the relative energy of the species with respect to the reactants. Since the simulations reflect crossed molecular beam experiments at the zero-pressure limit, only a single internal energy level is considered. Once all RRKM rate constants are obtained, product branching ratios are calculated by solving the kinetic equations under the steady-state approximation.

Details of the calculated rate constants and branching ratios, which depend on the initially formed reaction intermediate, are provided Table S2 and S3.

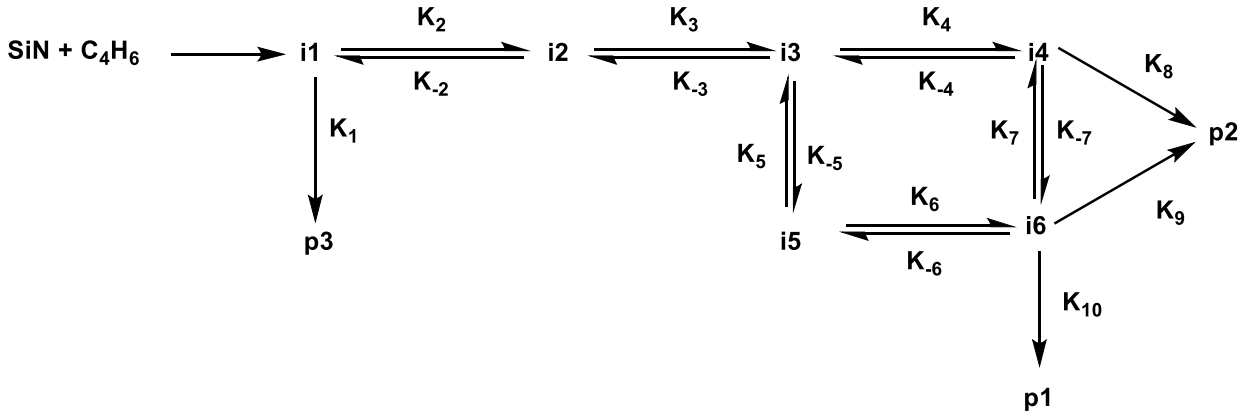

Table S2. RRKM rate constants (s^{-1}) for the reaction of silicon nitride radicals (SiN) with 1,3 butadiene (C_4H_6) computed with B2PLYP-D3(BJ)/Def2-TZVPP zero-point energy corrected CCSD(T)-F12/cc-pVTZ-F12 energies, and B2PLYP-D3(BJ)/Def2-TZVPP harmonic frequencies at collision energies of 0.0 kJ mol^{-1} and 24 kJ mol^{-1} relative to the entrance channel.

Rate Constant	At 0.0 kJ mol^{-1}	At 24 kJ mol^{-1}
K_1	2.37 X 10^5	2.28 X 10^6
K_2	3.68 X 10^{10}	5.42 X 10^{10}
K_{-2}	1.36 X 10^{11}	1.98 X 10^{11}
K_3	4.37 X 10^{10}	5.75 X 10^{10}
K_{-3}	1.75 X 10^{12}	2.04 X 10^{12}
K_4	6.49 X 10^2	2.72 X 10^4
K_{-4}	1.57 X 10^2	7.64 X 10^3
K_5	1.16 X 10^9	2.92 X 10^9
K_{-5}	2.46 X 10^5	9.63 X 10^5
K_6	3.37 X 10^9	4.97 X 10^9
K_{-6}	3.88 X 10^9	6.32 X 10^9
K_7	4.73 X 10^5	3.35 X 10^6
K_{-7}	4.77 X 10^2	5.01 X 10^3
K_8	9.45 X 10^8	2.48 X 10^9
K_9	2.83 X 10^6	1.07 X 10^7
K_{10}	1.57 X 10^8	3.67 X 10^8

Table S3. Statistical branching ratios (%) for the products of the reaction between Silicon nitride radical and 1,3 butadiene at the collision energy of 0.0 kJ mol^{-1} and 24.0 kJ mol^{-1}.

	Branching ratio (%)	
Products	**At 0.0 kJ mol^{-1}**	**At 24.0 kJ mol^{-1}**
p1	95.3	88.1
p2	1.7	2.6
p3	3.0	9.3

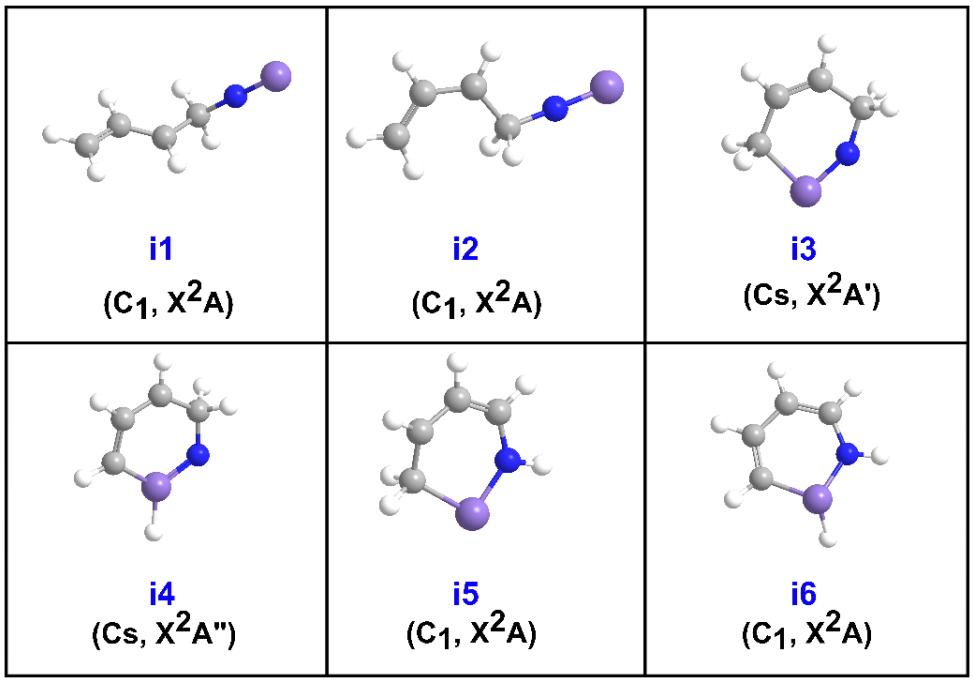

Figure S1. Optimized geometry of the intermediates for the reaction between silicon nitride radical and 1,3 butadiene at the B2PLYP-D3(BJ)/ Def2-TZVPP level of theory.

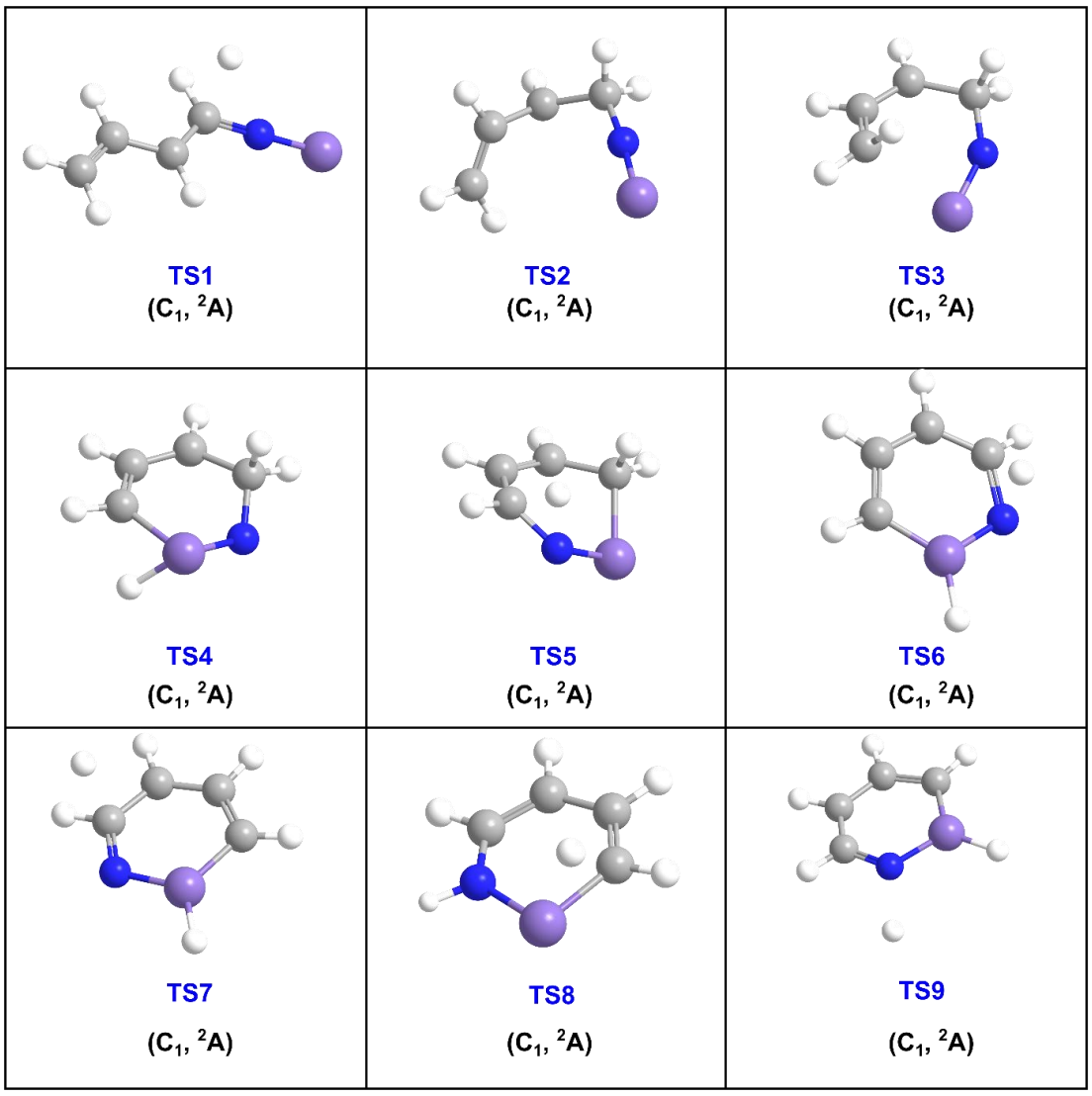

Figure S2. Optimized geometry of the transition states for the reaction between silicon nitride radical and 1,3 butadiene at the B2PLYP-D3(BJ)/ Def2-TZVPP level of theory.

Table S4. Kinetic bond order (KBO, kJ/mol) and bond order (BO) of the QUAO pairs of **p1-3**. Only interactions with BO > 0.2 and KBO > -4 kJ/mol. Note that the averages of KBOs and BOs of $C_{C\sigma} - C_{C\sigma}$ and $H_{C\sigma} - C_{H\sigma}$ are reported. The labels of atom numbers are depicted in **Figure S3**.

Interaction type	QUAO pair	p1		p2		p3	
		KBO	BO	KBO	BO	KBO	BO
$E - E\ \sigma$	$C_{4_{N\sigma}} - N_{C_4\sigma}$	-255	0.97	-259	0.98	-268	0.97
	$C_{C\sigma} - C_{C\sigma}$	-228	0.99	-223	0.98	-228	0.99
	$Si_{N\sigma} - N_{Si\sigma}$	-112	0.81	-128	0.89	-109	0.87
	$Si_{C_1\sigma} - C_{1_{Si\sigma}}$	-111	0.92	-115	0.92		
$E - H\ \sigma$	$H_{C\sigma} - C_{H\sigma}$	-159	0.97	-158	0.97	-158	0.98
	$H'_{N\sigma} - N_{H'\sigma}$	-177	0.95				
	$H'_{Si\sigma} - Si_{H'\sigma}$			-105	0.97		
$E - E\ \pi$	$C_{1_{C_2Si\pi}} - C_{2_{C_1C_3\pi}}$	-81	0.81	-64	0.69	-96	0.93
	$C_{3_{C_4C_2\pi}} - C_{4_{C_3N\pi}}$	-77	0.78	-61	0.65	-89	0.87
	$C_{2_{C_1C_3\pi}} - C_{3_{C_4C_2\pi}}$	-42	0.50	-59	0.64	-61	0.78
	$N_{C_4Si\pi} - C_{4_{C_3N\pi}}$	-49	0.53	-71	0.68	-64	0.81
	$N_{C_4Si\pi} - Si_{NC_1\pi}$	-37	0.53	-44	0.61		
	$Si_{NC_1\pi} - C_{1_{C_2Si\pi}}$	-30	0.49	-41	0.63		
	$C_{1_{C_2\pi}} - C_{2_{C_1\pi}}$					-96	0.93
	$C_{3_{C_4\pi}} - C_{4_{C_3\pi}}$					-89	0.87
	$N_{Si\pi} - Si_{N\pi}$					-61	0.78
	$N_{Si\pi'} - Si_{N\pi'}$ [a]					-64	0.81
Hyper conjugation	$N_{SiC_4\pi} - C_{3_{C_4C_2\pi}}$	-8	0.22				
	$Si_{C_1\sigma} - N_{lp}$			-13	0.22		
Weak $\pi - \pi$	$N_{Si\pi} - C_{4_{C_3\pi}}$					-33	0.38
	$C_{2_{C_1\pi}} - C_{3_{C_4\pi}}$					-28	0.35

[a] $N_{Si\pi'} - Si_{N\pi'}$ of **p3** is the π bond that is perpendicular to the molecular plane.

Table S5. Percentages of s and p characters and electron occupations (Occ.) of σ and lone-pair QUAOs of **p1-3**.

p1				p2				p3			
Orbital	%s	%p	Occ.	Orbital	%s	%p	Occ.	Orbital	%s	%p	Occ.
$C_{C\sigma}$	31	69	1.00	$C_{C\sigma}$	31	69	1.00	$C_{C\sigma}$	32	68	1.00
$C_{4_{N\sigma}}$	26	74	0.85	$C_{4_{N\sigma}}$	29	71	0.87	$C_{4_{N\sigma}}$	26	74	0.83
$C_{1_{Si\sigma}}$	34	66	1.34	$C_{1_{Si\sigma}}$	32	68	1.29				
$N_{C_4\sigma}$	31	69	1.17	$N_{C_4\sigma}$	33	67	1.12	$N_{C_4\sigma}$	39	61	1.18
$N_{Si\sigma}$	37	63	1.56	$N_{Si\sigma}$	40	60	1.42	$N_{Si\sigma}$	57	43	1.49
$Si_{N\sigma}$	11	89	0.44	$Si_{N\sigma}$	29	71	0.58	$Si_{N\sigma}$	19	81	0.51
$Si_{C_1\sigma}$	19	81	0.66	$Si_{C_1\sigma}$	35	65	0.74				
$C_{H\sigma}$	26	74	1.14	$C_{H\sigma}$	27	73	1.15	$C_{H\sigma}$	27	73	1.14
$N_{H'\sigma}$	23	77	1.28	$Si_{H'\sigma}$	36	64	0.89				
$H_{C\sigma}$	100	0	0.86	$H_{C\sigma}$	100	0	0.86	$H_{C\sigma}$	100	0	0.86

$H'_{N\sigma}$	100	0	0.78	$H'_{Si\sigma}$	100	0	1.13				
Si_{lp}	63	37	1.99	N_{lp}	20	80	1.91	Si_{lp}	78	22	1.99

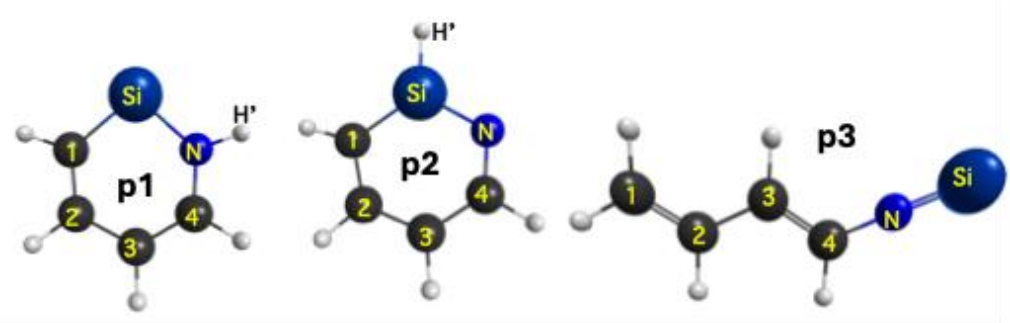

Figure S3. Atom numbers of C, N and Si for **p1-3**. Black represents carbon, whereas white represent hydrogen. Large blue represents silicon atom, while the smaller one represents nitrogen.

Table S6. Nucleus-Independent Chemical Shifts (NICS(0) and NICS(1)) calculated at B2PLYP/def2-TZVPP benchmarking with benzene for the characterization of aromaticity

Molecule	**Nucleus-Independent Chemical Shift (ppm)**	
	NICS(0)	**NICS(1)**
Benzene	-8.283	-10.082
p1	-3.255	-6.031
p2	-5.384	-7.449

Optimized Cartesian coordinates (Å) and vibrational frequencies (cm^{-1}) for all reactants, products, intermediates, and transition states involved in the reactions between silicon nitride radical and 1,3 butadiene at the B2PLYP-D3(BJ)/ Def2-TZVPP level of theory. The total energies of the final single-point calculation a the CCSD(T)-F12/cc-pVTZ level are also reported (in atomic units).

SiN

Si	0.000000	0.000000	-0.522865
N	0.000000	0.000000	1.047191

Frequency

1224

Energy: -343.641109232127

1, 3 Butadiene

C	1.840854	-0.117588	-0.00003
C	0.609552	0.401662	0.000091
C	-0.606004	-0.393353	0.000094
C	-1.837283	0.125932	-0.000046
H	1.996822	-1.187944	-0.000161
H	2.719171	0.509757	-0.000066
H	0.483981	1.478576	0.000169
H	-0.480476	-1.470266	0.000166
H	-2.715612	-0.501386	-0.000057
H	-1.993228	1.196286	-0.000159

Frequencies

168	273	519	537	780	905	938	939
996	1010	1057	1237	1320	1327	1424	1488
1651	1707	3155	3159	3163	3167	3253	3260

Energy: -155.765489207523

p1

C	0.552004	1.416853	-0.000007
C	1.578497	0.516026	-0.000008
C	1.359233	-0.882215	-0.000022
C	0.118404	-1.473084	0.000018
H	0.757443	2.479101	0.000028
H	2.588073	0.896731	0.00003
H	2.24697	-1.506968	-0.000053
H	0.107266	-2.558242	0.000057
Si	-1.48898	-0.578439	-0.000026
N	-0.75458	1.044987	-0.000007
H	-1.39319	1.826954	-0.000009

Frequencies

248	315	437	510	545	666	700	731	775
854	911	972	1001	1029	1115	1194	1263	1360
1417	1475	1558	1643	3133	3155	3189	3221	3583

Energy: -498.962594733668

p2

C	-0.141144	-1.468544	-0.00009
C	1.19841	-1.067442	-0.000004
C	1.651633	0.256992	-0.000052
C	0.807974	1.37346	0.000008
H	-0.370756	-2.524041	0.000065
H	1.958717	-1.840606	0.000104
H	2.717648	0.43371	-0.00006
H	1.284171	2.352589	0.000143
N	-0.525828	1.360508	-0.000061
Si	-1.275741	-0.121313	-0.000208
H	-2.737294	-0.200359	0.000155

Frequencies

282	357	430	480	506	569	738	763	820
851	881	926	991	993	1020	1125	1202	1304
1382	1444	1530	1575	2333	3105	3158	3208	3214

Energy: -498.949150831511

p3

C	-3.423028	0.637097	-0.000022
C	-2.399203	-0.227173	0.000082
C	-1.009181	0.156977	0.00007
C	-0.00196	-0.741583	-0.000107
H	-3.254905	1.70543	-0.00008
H	-4.447264	0.297129	-0.000088
H	-2.607697	-1.29154	0.000078
H	-0.768075	1.213134	0.000148
H	-0.236915	-1.802281	0.000004
N	1.318844	-0.423169	-0.000066
Si	2.853854	-0.087399	-0.00002

Frequencies

83	114	184	268	375	417	520	664	877
887	913	950	971	1041	1205	1285	1318	1342
1448	1503	1638	1679	3123	3155	3162	3182	3255

Energy: -498.925270369029

i1

C	-3.24266	-0.805153	-0.116192

C	-2.182277	-0.05556	0.3505
C	-1.081116	0.304199	-0.395977
C	0.054816	1.119768	0.135678
H	-3.262468	-1.164332	-1.134765
H	-4.076796	-1.053622	0.51976
H	-2.214222	0.277828	1.382504
H	-1.001004	-0.025664	-1.424633
H	-0.131437	1.367508	1.183396
N	1.301835	0.436253	0.011594
Si	2.642752	-0.346903	-0.166058
H	0.117486	2.069528	-0.406822

Frequencies

40	117	208	250	274	405	521	560	745	800
820	919	983	1011	1135	1196	1244	1294	1327	1385
1458	1489	1519	1529	2998	3058	3164	3173	3181	3278

Energy: -499.493692049744

i2

C	-3.09317	-0.27848	0.913631
C	-2.48384	0.260936	-0.19628
C	-1.11874	0.391148	-0.38952
C	-0.08731	-0.03865	0.611119
H	-2.52454	-0.65911	1.748578
H	-4.16749	-0.33904	0.981685
H	-3.12321	0.621879	-0.99258
H	-0.7472	0.84374	-1.29693
H	-0.34565	-1.02728	1.003842
N	1.225186	-0.07041	0.067047
Si	2.65798	-0.10878	-0.55348
H	-0.10945	0.639985	1.472864

Frequencies

84	119	225	270	334	432	547	557	667	816
829	969	1008	1014	1051	1192	1227	1259	1339	1439
1463	1481	1503	1547	2977	3027	3172	3176	3217	3274

Energy: -499.492875860329

i3

C	1.239104	1.012877	-0.09568
C	-0.27221	1.078351	0.053274
C	-1.08159	0.022962	0.105829
C	-0.73373	-1.43081	0.035402
H	1.697262	1.52813	0.755991
H	1.526518	1.570608	-0.99405

H	-0.68929	2.076077	0.118737
H	-2.14273	0.230211	0.214499
H	-1.22497	-1.92165	-0.80898
Si	1.213775	-1.88763	-0.16471
N	1.628798	-0.33434	-0.16643
H	-1.0567	-1.96579	0.932417

Frequencies

93	204	303	367	411	515	593	735	740	803
869	955	961	1026	1095	1137	1238	1243	1301	1344
1403	1444	1499	1702	2982	3021	3026	3076	3128	3177

Energy: -499.483403113881

i4

C	0.38416	1.502555	0.000748
C	-1.01191	1.282738	-0.00449
C	-1.62446	0.053594	-0.00607
C	-0.96063	-1.29032	-0.00284
H	0.752038	2.517847	0.001658
H	-1.66163	2.150691	-0.00749
H	-2.70771	0.032585	-0.01019
H	-1.35591	-1.85143	-0.8651
N	0.477946	-1.38257	0.002891
Si	1.338921	-0.01843	0.005471
H	2.805317	-0.03486	0.0114
H	-1.36279	-1.8508	0.856617

Frequencies

157	279	411	440	459	550	642	731	740	785
828	884	942	965	1009	1063	1187	1234	1262	1294
1345	1427	1454	1534	2316	2928	2937	3156	3181	3215

Energy: -499.492725547753

i5

C	1.076686	-1.187	-0.16013
C	1.726752	0.034034	0.014503
C	1.081448	1.234378	0.160834
C	-0.37173	1.417999	-0.12278
H	1.636671	-2.09738	-0.30917
H	2.805278	0.003517	0.081614
H	1.66754	2.102515	0.433013

H	-0.52372	1.576444	-1.20383
Si	-1.5092	-0.08777	0.263423
N	-0.28812	-1.31126	-0.00054
H	-0.59936	-2.27042	0.038722
H	-0.76464	2.319525	0.348776

Frequencies

17	265	376	462	509	572	627	669	698	722
769	898	939	960	1031	1110	1167	1215	1234	1346
1424	1431	1510	1543	2925	3077	3172	3198	3220	3586

Energy: -499.523985515262

i6

C	-0.11766	-1.46116	-0.1004
C	1.182398	-1.08868	0.058382
C	1.667127	0.260154	0.011119
C	0.857147	1.34095	-0.15023
H	-0.34929	-2.51711	-0.04116
H	1.925003	-1.85425	0.255844
H	2.722874	0.440263	0.138005
H	1.27938	2.3367	-0.14692
N	-0.49785	1.266318	-0.30496
Si	-1.40477	-0.23411	-0.552
H	-2.5887	-0.20775	0.359739
H	-0.95505	2.158135	-0.40107

Frequencies

157	318	396	477	497	582	650	679	699	736
771	809	910	957	976	1002	1121	1197	1271	1380
1404	1480	1566	1650	2125	3154	3181	3190	3227	3619

Energy: -499.536628906137

TS1

C	-2.24735	-0.77951	-0.15052
C	-1.23293	0.052982	0.10132
C	0.133389	-0.19599	-0.27778
C	1.146741	0.659753	0.021169
H	-2.0894	-1.71576	-0.66813
H	-3.25646	-0.54543	0.151577
H	-1.42927	0.981718	0.62543
H	0.368479	-1.12293	-0.78522
H	1.35607	0.205623	1.85925
N	2.431486	0.494913	-0.41548

Si	3.911249	0.332215	-0.90001
H	0.907997	1.632422	0.438388

Frequencies

-956.32	80.47	103.56	156.31	262.79	294.15	413.33	468.87	486.65	516.04
663.51	880.98	890.91	936.34	972.76	983.09	1045.83	1206.22	1275.96	1313.75
1350.48	1457.92	1518.54	1625.98	1707.73	3140.36	3152.13	3164.69	3189.87	3259.11

Energy: -499.420970800882

TS2

C	-1.63421	-0.99266	-0.4964
C	-1.18162	0.14096	0.03697
C	-0.00631	0.878959	-0.42934
C	1.329657	0.750367	0.246438
H	-1.14494	-1.44666	-1.34631
H	-2.5082	-1.48809	-0.09871
H	-1.71316	0.551655	0.89575
H	-0.14845	1.744755	-1.06321
H	1.334776	1.357926	1.164313
N	1.6677	-0.58767	0.57729
Si	1.909461	-2.09303	0.915359
H	2.095306	1.18348	-0.40216

Frequencies

-203	80	110	237	248	302	454	530	707	788
874	967	982	1018	1048	1122	1245	1310	1326	1363
1460	1470	1491	1680	2936	3038	3074	3155	3186	3254

Energy: -499.468780506034

TS3

C	-0.89606	-1.33002	0.240653
C	-1.18392	0.03866	-0.075
C	-0.31174	1.068554	-0.04093
C	1.194116	0.91055	0.05671
H	-0.31476	-1.55261	1.123802
H	-1.63009	-2.08148	-0.01797
H	-2.1963	0.255064	-0.39831
H	-0.68118	2.076632	-0.17722
H	1.508353	1.061875	1.098925
N	1.626984	-0.35329	-0.41739

Si	1.22954	-1.81707	-0.88151
H	1.655062	1.723128	-0.51177

Frequencies

-301	121	241	270	375	444	577	681	725	797
852	908	946	991	1026	1111	1227	1250	1337	1384
1404	1485	1501	1581	2969	3030	3141	3152	3191	3239

Energy: -499.474267123946

TS4

C	-0.89381	1.092406	0.443072
C	0.524486	1.086896	0.176949
C	1.169096	-0.07432	-0.05152
C	0.490921	-1.42269	-0.13781
H	-1.32193	2.015535	0.822379
H	1.088288	2.010932	0.190601
H	2.244926	-0.06943	-0.1765
H	0.423044	-1.81489	0.894257
N	-0.81597	-1.35153	-0.74049
Si	-1.97386	-0.3303	0.076481
H	-2.07542	0.971645	-0.81889
H	1.140218	-2.11426	-0.67853

Frequencies

-949	112	231	355	422	456	634	661	732	771
796	893	966	977	1031	1069	1088	1156	1223	1323
1349	1431	1468	1649	1812	2891	3044	3152	3174	3192

Energy: -499.410889689711

TS5

C	-1.02552	1.073818	-0.15768
C	0.392191	1.069016	0.309875
C	1.167497	-0.03753	0.267856
C	0.616339	-1.32458	-0.08452
H	-1.51031	2.032929	0.001021
H	0.819579	1.991405	0.681209
H	2.219424	0.013399	0.510985
H	1.277377	-2.16973	-0.24181
N	-0.74332	-1.64999	0.18874
Si	-1.87919	-0.41575	0.745297
H	-1.06963	0.847478	-1.23199
H	-0.26445	-1.43047	-0.98898

Frequencies

-1649	113	270	350	425	501	594	650	683	703
770	856	922	959	976	1010	1079	1134	1165	1234
1366	1433	1456	1614	2230	2976	3132	3143	3174	3204

Energy: -499.421872417199

TS6

C	-0.76206	1.363304	0.203632
C	0.666833	1.172364	0.222993
C	1.317042	-0.01554	0.005058
C	0.700715	-1.27932	-0.24042
H	-1.15837	2.350188	0.385557
H	1.284333	2.03983	0.419668
H	2.398515	-0.01673	0.026105
H	-0.14694	-1.83562	0.557712
N	-0.76911	-1.45351	-0.43916
Si	-1.67962	-0.06327	-0.16323
H	-3.13319	-0.17961	-0.3062
H	1.281862	-2.08209	-0.67172

Frequencies

-2020	215	287	409	442	460	531	638	701	725
774	811	833	927	937	972	980	1026	1126	1220
1321	1362	1455	1596	2249	2331	3163	3179	3202	3224

Energy: -499.423893207265

TS7

C	-0.75874	1.420507	-0.01127
C	0.591975	1.144675	0.236187
C	1.153661	-0.12633	0.332487
C	0.426281	-1.33092	0.171518
H	-1.07857	2.450276	-0.07217
H	1.266584	1.983339	0.366502
H	2.216418	-0.2107	0.508686
H	0.958872	-2.25289	0.397909
N	-0.90582	-1.43272	0.021885
Si	-1.75504	-0.02538	-0.14823
H	-3.20406	-0.0636	-0.35362
H	1.088429	-1.55626	-1.44988

Frequencies

-1033	254	296	389	431	463	507	526	633	735
762	834	859	877	938	996	1017	1063	1119	1202
1296	1373	1436	1517	1567	2332	3099	3162	3207	3211

Energy: -499.442381128404

TS8

C	-0.75095	1.271402	0.261662
C	0.640511	1.141474	0.268524
C	1.268796	-0.11333	0.107598
C	0.587038	-1.29314	-0.04664
H	-1.46836	0.899925	-1.09978
H	1.266647	2.020003	0.34981
H	2.347134	-0.16571	0.099377
H	1.14412	-2.21451	-0.15503
N	-0.77037	-1.39846	-0.06224
Si	-2.01042	-0.08346	0.103284
H	-1.14916	2.278842	0.33987
H	-1.10497	-2.34304	-0.16644

Frequencies

-1055	194	329	416	499	528	608	630	681	691
778	863	908	958	999	1037	1114	1193	1265	1345
1405	1458	1510	1551	1622	3148	3178	3183	3220	3609

Energy: -499.486219506751

TS9

C	-0.00926	-0.01962	0.116713
C	1.375945	0.000474	-0.06055
C	2.172756	1.153334	-0.06165
C	1.689258	2.446532	0.101682
H	-0.52538	-0.96863	0.117755
H	1.885056	-0.94461	-0.20933
H	3.239249	1.036792	-0.19098
H	2.403195	3.265189	0.072905
N	0.401575	2.804001	0.265355
Si	-0.72636	1.568274	0.347673
H	-2.14078	1.90186	0.509183
H	0.019017	4.095842	-0.60441

Frequencies

-1146	203	246	364	415	462	481	506	572	725
745	816	851	872	921	992	998	1011	1125	1199
1288	1372	1446	1543	1571	2344	3127	3160	3197	3210

Energy: -499.442863721213

References

[1] V. S. Krasnoukhov, V. N. Azyazov, A. M. Mebel, S. Doddipatla, Z. Yang, S. Goettl, R. I. Kaiser,"Combined Crossed Molecular Beams and Ab Initio Study of the Bimolecular Reaction of Ground State Atomic Silicon (Si; ^3P) with Germane (GeH_4; X^1A_1)". *ChemPhysChem* **2021**, *22*, 1497-1504.

[2] R. I. Kaiser, P. Maksyutenko, C. Ennis, F. Zhang, X. Gu, S. P. Krishtal, A. M. Mebel, O. Kostko, M. Ahmed,"Untangling the chemical evolution of Titan's atmosphere and surface–from homogeneous to heterogeneous chemistry". *Faraday Discuss.* **2010**, *147*, 429-478.

[3] R. I. Kaiser,"Experimental investigation on the formation of carbon-bearing molecules in the interstellar medium via neutral-neutral reactions". *Chem. Rev.* **2002**, *102*, 1309-1358.

[4] G. O. Brink,"Electron bombardment molecular beam detector". *Rev. Sci. Instrum.* **1966**, *37*, 857-860.

[5] N. Daly,"Scintillation type mass spectrometer ion detector". *Rev. Sci. Instrum.* **1960**, *31*, 264-267.

[6] M. F. Vernon, *Molecular beam scattering*, University of California, Berkeley, **1983**.

[7] P. S. Weiss, in *Ph.D. Dissertation*, University of California, Berkeley, CA, **1986**.

[8] F. Neese,"Software update: The ORCA program system—Version 5.0". *WIREs Comput. Mol. Sci.* **2022**, *12*, e1606.

[9] S. Grimme,"Semiempirical hybrid density functional with perturbative second-order correlation". *J. Chem. Phys.* **2006**, *124*, 034108.

[10] S. Grimme, S. Ehrlich, L. Goerigk,"Effect of the damping function in dispersion corrected density functional theory". *J. Comput. Chem.* **2011**, *32*, 1456-1465.

[11] A. D. Becke, E. R. Johnson,"A density-functional model of the dispersion interaction". *J. Chem. Phys.* **2005**, *123*, 154101.

[12] F. Weigend, R. Ahlrichs,"Balanced basis sets of split valence, triple zeta valence and quadruple zeta valence quality for H to Rn: Design and assessment of accuracy". *Phys. Chem. Chem. Phys.* **2005**, *7*, 3297-3305.

[13] P. v. R. Schleyer, C. Maerker, A. Dransfeld, H. Jiao, N. J. R. van Eikema Hommes,"Nucleus-Independent Chemical Shifts: A Simple and Efficient Aromaticity Probe". *J. Am. Chem. Soc.* **1996**, *118*, 6317-6318.

[14] Z. Chen, C. S. Wannere, C. Corminboeuf, R. Puchta, P. v. R. Schleyer,"Nucleus-Independent Chemical Shifts (NICS) as an Aromaticity Criterion". *Chem. Rev.* **2005**, *105*, 3842-3888.

[15] R. Ditchfield,"Self-consistent perturbation theory of diamagnetism". *Mol. Phys.* **1974**, *27*, 789-807.

[16] G. L. Stoychev, A. A. Auer, F. Neese,"Efficient and Accurate Prediction of Nuclear Magnetic Resonance Shielding Tensors with Double-Hybrid Density Functional Theory". *J. Chem. Theory Comput.* **2018**, *14*, 4756-4771.

[17] T. B. Adler, G. Knizia, H.-J. Werner,"A simple and efficient CCSD (T)-F12 approximation". *J. Chem. Phys.* **2007**, *127*, 221106-221110

[18] G. Knizia, T. B. Adler, H.-J. Werner,"Simplified CCSD (T)-F12 methods: Theory and benchmarks". *J. Chem. Phys.* **2009**, *130*, 054104-054124

[19] K. A. Peterson, T. B. Adler, H.-J. Werner,"Systematically convergent basis sets for explicitly correlated wavefunctions: The atoms H, He, B–Ne, and Al–Ar". *J. Chem. Phys.* **2008**, *128*, 084102.

[20] H. Werner, P. Knowles, G. Knizia, F. Manby, M. Schütz, P. Celani, W. Györffy, D. Kats, T. Korona, R. Lindh,"MOLPRO, version 2015.1, a package of ab initio programs". *University of Cardiff Chemistry Consultants (UC3): Cardiff, Wales, UK* **2015**.

[21] E. B. Guidez, M. S. Gordon, K. Ruedenberg,"Why is Si_2H_2 not linear? An intrinsic quasi-atomic bonding analysis". *J. Am. Chem. Soc.* **2020**, *142*, 13729-13742.

[22] A. C. West, M. W. Schmidt, M. S. Gordon, K. Ruedenberg,"A comprehensive analysis in terms of molecule-intrinsic quasi-atomic orbitals. IV. Bond breaking and bond forming along the dissociative reaction path of dioxetane". *J. Phys. Chem. A* **2015**, *119*, 10376-10389.

[23] A. C. West, M. W. Schmidt, M. S. Gordon, K. Ruedenberg,"A comprehensive analysis in terms of molecule-intrinsic, quasi-atomic orbitals. III. The covalent bonding structure of urea". *J. Phys. Chem. A* **2015**, *119*, 10368-10375.

[24] A. C. West, M. W. Schmidt, M. S. Gordon, K. Ruedenberg,"A comprehensive analysis in terms of molecule-intrinsic, quasi-atomic orbitals. II. Strongly correlated MCSCF wave functions". *J. Phys. Chem. A* **2015**, *119*, 10360-10367.
[25] A. C. West, M. W. Schmidt, M. S. Gordon, K. Ruedenberg,"A comprehensive analysis of molecule-intrinsic quasi-atomic, bonding, and correlating orbitals. I. Hartree-Fock wave functions". *J. Chem. Phys.* **2013**, *139*, 234107.
[26] A. C. West, J. J. Duchimaza-Heredia, M. S. Gordon, K. Ruedenberg,"Identification and characterization of molecular bonding structures by ab initio quasi-atomic orbital analyses". *J. Phys. Chem. A* **2017**, *121*, 8884-8898.
[27] D. D. A. Cruz, K. N. Ferreras, T. Harville, G. Schoendorff, M. S. Gordon,"Analysis of bonding motifs in unusual molecules I: planar hexacoordinated carbon atoms". *Phys. Chem. Chem. Phys.* **2024**, *26*, 21395-21406.
[28] J. I. Steinfeld, J. S. Francisco, W. L. Hase, *Chemical kinetics and dynamics, Vol. 2*, Prentice Hall Upper Saddle River, NJ, **1999**.
[29] H. Eyring, S. H. Lin, *Basic chemical kinetics*, John Wiley & Sons, Inc., **1980**.
[30] C. He, L. Zhao, A. M. Thomas, A. N. Morozov, A. M. Mebel, R. I. Kaiser,"Elucidating the chemical dynamics of the elementary reactions of the 1-propynyl radical (CH_3CC; X^2A_1) with methylacetylene (H_3CCCH; X^1A_1) and allene (H_2CCCH_2; X^1A_1)". *J. Phys. Chem. A* **2019**, *123*, 5446-5462.
[31] V. Kislov, T. Nguyen, A. Mebel, S. Lin, S. Smith,"Photodissociation of benzene under collision-free conditions: An ab initio/Rice–Ramsperger–Kassel–Marcus study". *J. Chem. Phys.* **2004**, *120*, 7008-7017.